Electronic Supplementary Material (ESI) for ChemComm.

Cryogenic Activity and Stability of Benzaldehyde Lyase Enzyme in Lipidic Mesophases-Nanoconfined Water

Tao Zhou,[1] Yang Yao,[1] Qin Zhang[1,2] and Raffaele Mezzenga[1,3]*

1Department of Health Sciences and Technology, ETH Zürich, 8092 Zurich, Switzerland

2 Institut des Sciences et Ingénierie Chimiques, EPFL, 1015 Lausanne, Switzerland

3 Department of Materials, ETH Zurich, 8093 Zürich, Switzerland

*Author for correspondence: E-mail: Raffaele.mezzenga@hest.ethz.ch

Contents

1. Materials and Methods

1.1 Materials

Phytantriol was purchased from DSM. 2-Naphthaldehyde, dimethyl sulfoxide (DMSO), $MgSO_4$, Thiamine-diphosphate (ThDP), potassium phosphate buffer and deuterium oxide were purchased from Sigma and used without further purification. The buffer used in this work was potassium phosphate buffer (50 mmol/L, pH=7.0) containing $MgSO_4$ (2.5 mmol/L) and ThDP (0.3 mmol/L). Benzaldehyde lyase (BAL) was kindly provided by Prof. Donald Hilvert group.

1.2 Mesophase sample preparation

The sample was prepared by using a two connected Hamilton RN syringes setup. One was loaded with desired amount of phytantriol and naphthaldehyde, while the second one was loaded with the desired amount of BAL and buffer. The reaction thus was initiated only when mixing occurs. Once the mixture becomes homogeneous, it will be transferred to three sealed vials and stored separately at 25 ℃, 4 ℃ and -5 ℃. For all the samples, the final naphthaldehyde

concentration (100 mM) and the final BAL concentration (0.42 mg/mL) were the same. The experiment was repeated 3 times for each mesophase.

1.3 Enzymatic reaction in solution

Desired amount of naphthaldehyde was dissolved in DMSO, and the concentrated BAL solution was diluted with buffer then added to naphthaldehyde solution, then it was kept at 25 ℃. The final concentration of naphthaldehyde and BAL were 2.5 mM, 0.01 mg/mL, respectively. The ratio of DMSO and water is 1 to 4.

1.4 High Performance Liquid Chromatography (HPLC) measurement

HPLC measurement was carried out on Agilent 1200. 50 μL solution were injected and eluted with the following conditions: 59.5 vol.% water with 0.5% acetate acid, 40 vol.% acetonitrile, flow rate 1 mL/min^{-1}, detection at 254 nm. For the mesophase sample, 10 mg sample was dissolved in 990 mL ethanol before HPLC sampling. For solution sample, it was first centrifuged at 3300 r/min for 10 min and the supernatant was sampled without dilution. Naphthaldehyde dissolved in DMSO/H_2O (1:4) solutions with different concentrations were prepared and tested to get the calibration curve.

1.5 Small Angle X-ray Scattering (SAXS) measurement

SAXS was used to identify the phase and dimension of mesophases in different temperatures. Static SAXS patterns were acquired using a Bruker AXS Micro X-ray. The X-ray source was a well-collimated (2D-Kratky) beam of wavelength λ = 1.5418 Å from a microfocused source operating at 50 kV and 1000 μA. Diffracted X-rays were collected on a 2D Pilatus K100 detector. The scattering vector $q = (4\pi/\lambda)\sin\theta$, with 2θ, the scattering angle, was calibrated using silver behenate in the q-range from 0.03 to 0.6 Å^{-1}. Samples were placed inside a stainless steel cell between two thin, replaceable mica sheets and sealed by an O-ring, with a sample volume of 10 μL with a thickness around 1 mm. Scattered intensity was collected at 25 ℃, 4 ℃ and -5 ℃ for over 30 min for completely phase transition and good signal to noise ratio. Data were collected and azimuthally averaged using the Saxsgui software to yield 1D intensity versus scattering vector q. The lattice parameters and water channel dimeters are calculated as following:[1-4]

The lattice parameter a could be calculated using the following equation:

$$a = \frac{2\pi}{q}Q \tag{1}$$

where q is the measured scattering vector of the Bragg reflection and Q is the corresponding value in the specific spacing ratio. For the *Ia3d*, $\boldsymbol{Q} = \sqrt{6}, \sqrt{8}, \sqrt{14}, \sqrt{16}, \sqrt{20}$, and $\sqrt{22}$; For the *Pn3m*, $\boldsymbol{Q} = \sqrt{2}, \sqrt{3}, \sqrt{4}, \sqrt{6}, \sqrt{8}$, and $\sqrt{9}$;

The lipid length (l_{lip}) can be obtained by solving the following equation

$$\varphi_{lipid} = 2A_0\left(\frac{l_{lip}}{a}\right) + \frac{4}{3}\pi\chi\left(\frac{l_{lip}}{a}\right)^3 \quad (2)$$

where φ_{lipid} is the lipid volume fraction, A_0 is the minimal surface in a unit cell to (unit cell volume)$^{2/3}$ and χ is the Euler–Poincaré characteristic; For *Ia3d* phase, $A_0 = 3.091$, $\chi = -8$. For *Pn3m* phase, $A_0 = 1.919$, $\chi = -2$.

Then, the radius of water channel is obtained using the following equation

For *Ia3d* phase, $r = 0.248a - l_{lip}$ (3a)

For *Pn3m* phase, $r = 0.391a - l_{lip}$ (3b)

1.6 Fourier-Transform Infrared Spectroscopy (FTIR) measurement

FTIR experiments were conducted on a Varian 640 FTIR Spectrometer with a demountable transmission cell for liquid or gel sample. The light path was purged with nitrogen incessantly to avoid the interference of water vapor and CO_2. The background was obtained without placing sample cell and was subtracted automatically. Samples were placed between two CaF_2 windows. A 50 μm and 6 μm Teflon spacer were used for mesophase sample and solution sample respectively. Spectra from 1000 cm^{-1} to 4000 cm^{-1} were acquired by collecting 128 interferograms at 4 cm^{-1} resolution and averaged. The temperature of the sample cell was controlled by Julabo temperature regulator. For each measurement at each temperature, the background was remeasured and subtracted.

2. Support results

2.1 Structure characterization of LMs

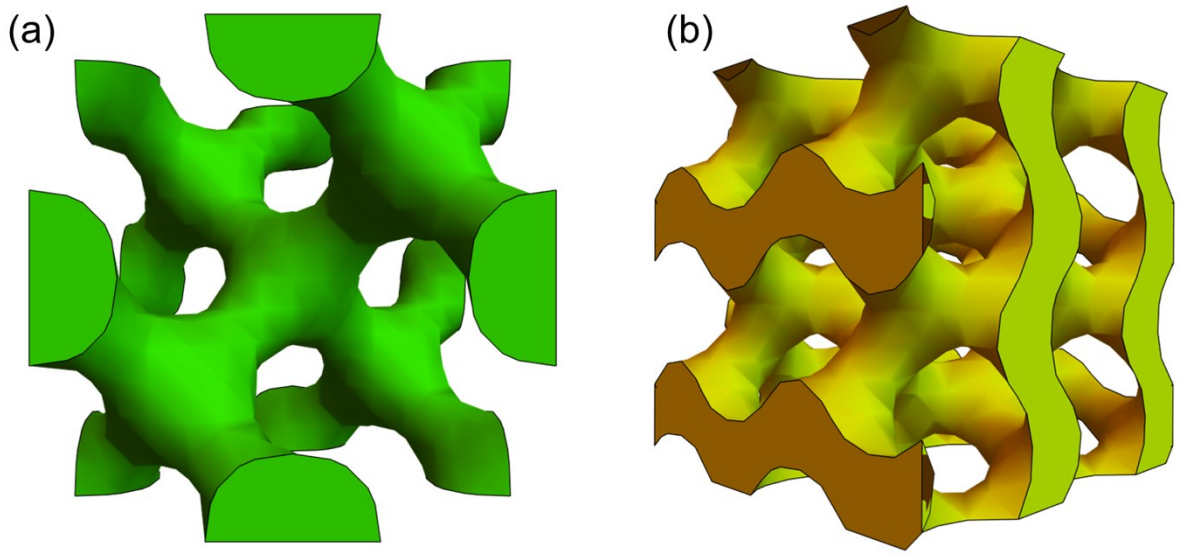

Figure S1. Schematic of (a) Pn3m lipidic mesophases and (b) Ia3d lipidic mesophases.

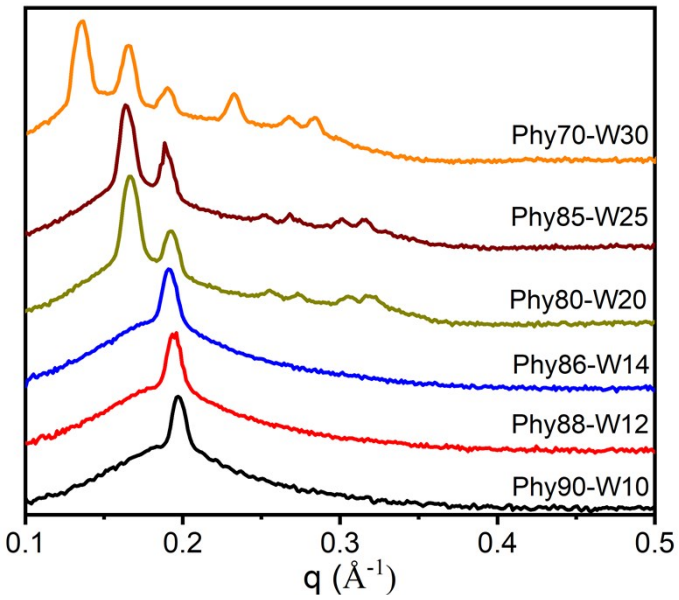

Figure S2. SAXS profiles at 25 ℃ of phytantriol-based lipid mesophases with different water content in the presence of both naphthaldehyde and BAL. In all the cases, the concentrations of naphthaldehyde and BAL in LMs were kept the same. All the measurements were carried out after the complement of reactions. Black: Phy90-W10, Lα; red: Phy88-W12, Lα; blue: Phy86-W14, Lα; dark yellow: Phy80-W20, Ia3d; wine: Phy85-W25, Ia3d; orange: Phy70-W30, Pn3m.

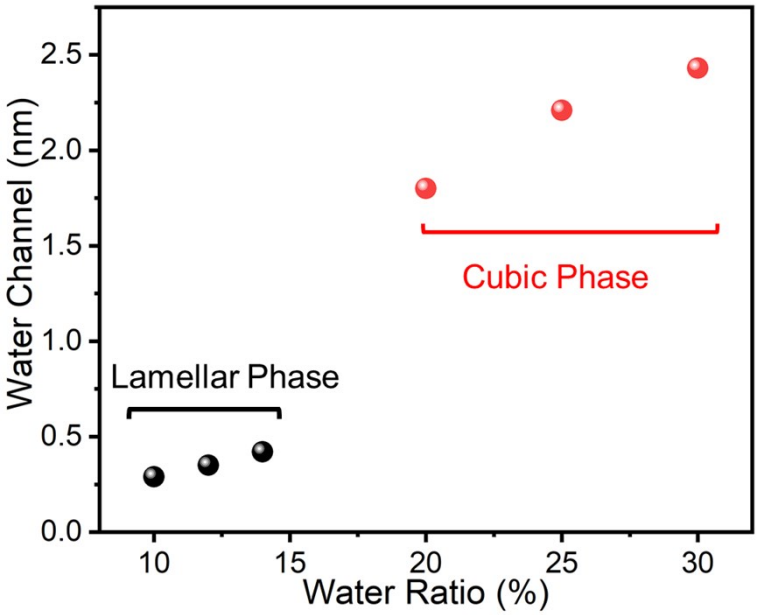

Figure S3. The size of water channel in LMs with different water ratio at 25 °C.

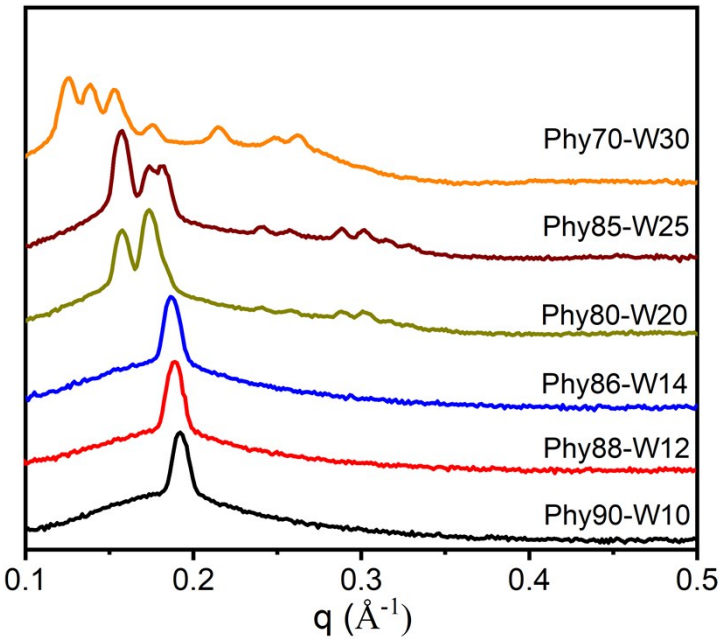

Figure S4. SAXS profiles at 4℃ of phytantriol-based lipid mesophases with different water content in the presence of both naphthaldehyde and BAL. In all the cases, the concentrations of naphthaldehyde and BAL in LMs were kept the same. All the measurements were carried out after the complement of reactions. Black: Phy90-W10, Lα; red: Phy88-W12, Lα; blue: Phy86-W14, Lα; dark yellow: Phy80-W20, Ia3d; wine: Phy85-W25, Ia3d; orange: Phy70-W30, mixture of Ia3d and Pn3m.

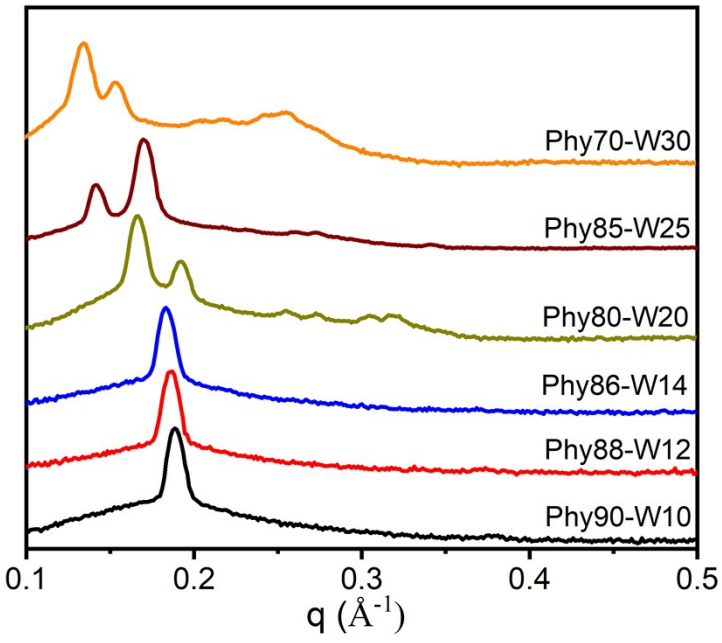

Figure S5. SAXS profiles at -5℃ of phytantriol-based lipidic mesophases with different water content in the presence of both naphthaldehyde and BAL. In all the cases, the concentrations of naphthaldehyde and BAL in LMs were kept the same. All the measurements were carried out after the complement of reactions. Black: Phy90-W10, Lα; red: Phy88-W12, Lα; blue: Phy86-W14, Lα; dark yellow: Phy80-W20, Ia3d; wine: Phy85-W25, Ia3d and Lα; orange: Phy70-W30, Ia3d.

2.2 Thermal study of water confined in LMs

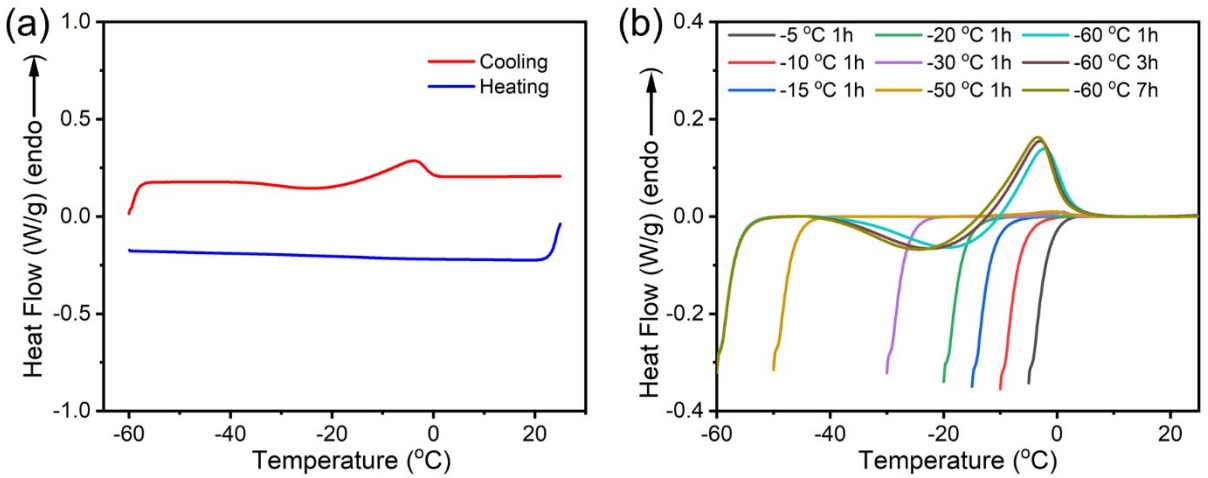

Figure S6. (a) DSC curves of Phy88-W12 in the presence of BAL enzyme and NA substrate obtained on cooling and heating modes with a rate of 5°C/min. (b) Melting curves of Phy88-W12 in the presence of BAL enzyme and NA substrate obtained following annealing at different temperatures as indicated.

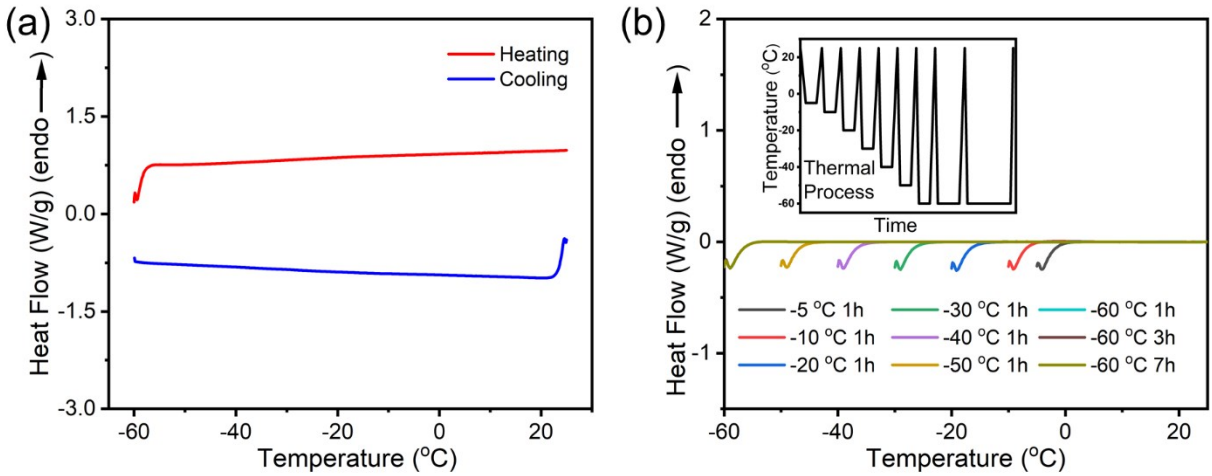

Figure S7. (a) DSC curves of Phy90-W10 in the presence of BAL enzyme and NA substrate obtained on cooling and heating modes with a rate of 5°C/min. (b) Melting curves of Phy90-W10 in the presence of BAL enzyme and NA substrate obtained following annealing at different temperatures as indicated. The inset of (b) shows the thermal process.Table 1. The melting enthalpy of water confined in Phy70-W30 in the presence of BAL enzyme and NA substrate after annealing at different temperatures for different times and the ratio of ice ($\Delta H/\Delta H_0$)

T (°C)	Annealing time	ΔH (J/g)	ΔH / ΔH_0
-20	1h	168.0	50.4%
-30	1h	172.7	51.8%
-40	1h	177.4	53.2%
-50	1h	177.5	53.2%
-60	1h	175.4	52.6%
-60	3h	174.7	52.4%
-60	7h	176.3	52.9%

Table 2. The melting enthalpy of water confined in Phy88-W12 in the presence of BAL enzyme and NA substrate after annealing at different temperatures for different times and the ratio of ice ($\Delta H/\Delta H_0$)

T (°C)	Annealing time	ΔH (J/g)	ΔH / ΔH_0
-30	1h	1.945	0.58%
-50	1h	4.825	1.45%
-60	1h	53.8	16.13%
-60	3h	64.1	19.21%
-60	7h	70.25	21.06%

2.3 Kinetics study of enzymatic reactions confined in LMs

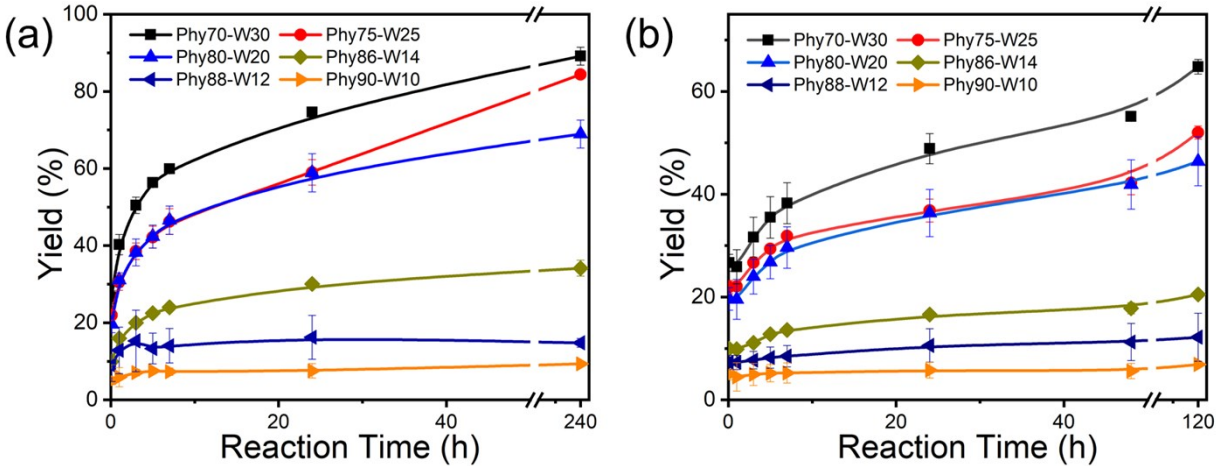

Figure S8. Kinetic curves of the enzymatic reaction in LMs with different water ratio at (a) 4 °C and (b) -5 °C.

2.4 FTIR characterization of the secondary structure of enzyme BAL

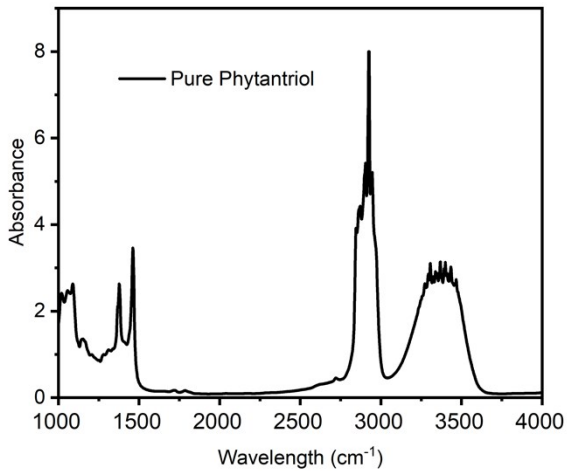

Figure S9. FTIR spectrum of pure phytantriol.

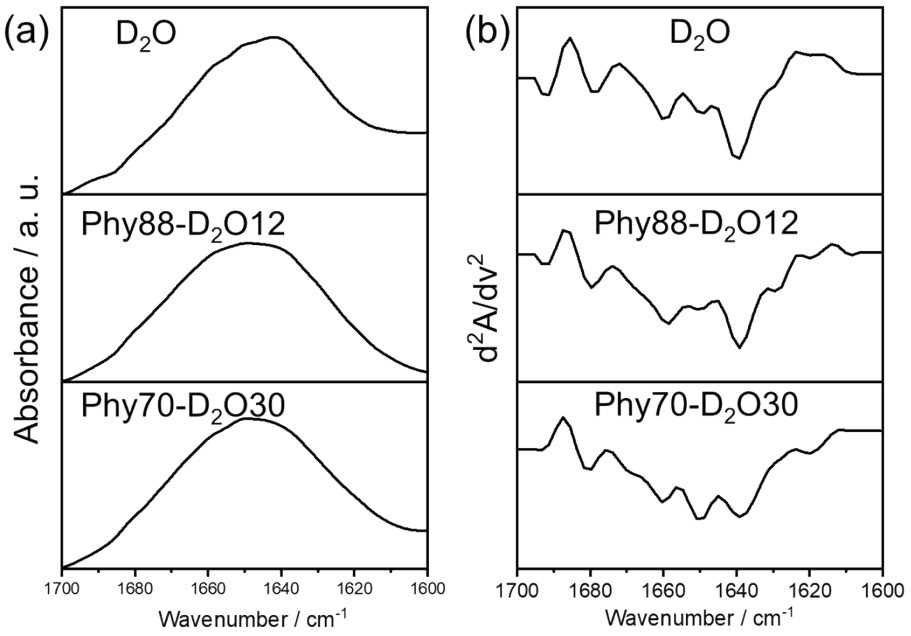

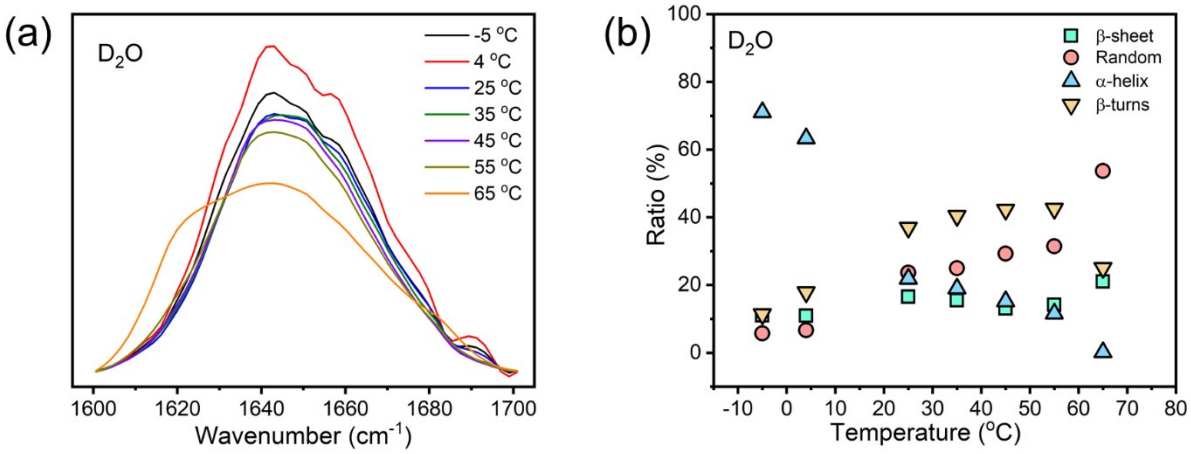

Figure S10. (a) FTIR spectra for BAL in D_2O, Phy88-D_2O12 and Phy70-D_2O30. (b) The secondary derivative of the FTIR spectrum.

Figure S11 (a) FTIR spectrum of BAL in D_2O at different temperatures; (b) Temperature dependence of the secondary structural distribution of BAL in D_2O.

It is clear that the enzyme BAL is also sensitive to the increase of the temperature. The α-helix structure ratio decreases with increasing the temperature, while the random structure increases. The dramatical change of secondary structural distribution is observed while the temperature is enhanced to 65 °C, indicating the heat denaturation occurs.

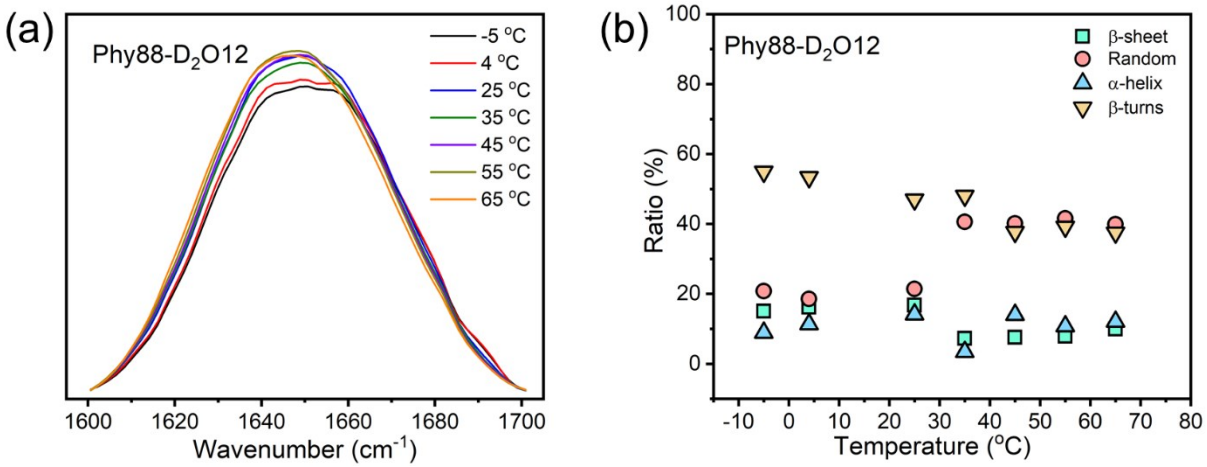

Figure S12 (a) FTIR spectrum of BAL in Phy88-D_2O12 at different temperatures; (b) Temperature dependence of the secondary structural distribution of BAL in Phy88-D_2O12.

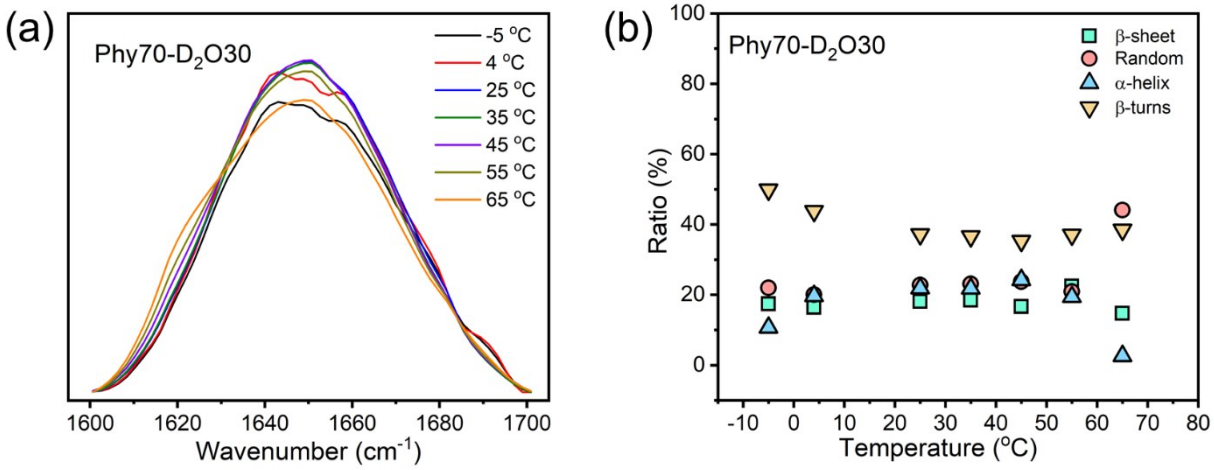

The structure of enzyme BAL confined in Phy88-D_2O12 remains relatively stable, except the clear change at 35 °C. While increasing the temperature from 25 °C to 35°C, the lamellar phase changes to reverse micelle. This structural transition of the host is deduced to induce the BAL structural change. This shows that the reverse micelle is not a good host for enzymes, compared with lamellar and cubic mesophases. Figure S13 (a) FTIR spectrum of BAL in Phy70-D_2O30 at different temperatures; (b) Temperature dependence of the secondary structural distribution of BAL in Phy70-D_2O30.

Enzyme BAL in Phy70-D_2O30 remains stable up to 55 °C. The heat denaturation would occur while the temperature is enhanced to 65 °C.

Table 3. The secondary structural distribution of BAL in D_2O Phy88-D_2O12 and Phy70-D_2O30

T / °C	D2O				Phy88-D2O12				Phy70-D2O30			
	β-sheet	Random	α-helix	β-turns	β-sheet	Random	α-helix	β-turns	β-sheet	Random	α-helix	β-turns
-5	11.03379	5.71194	71.04982	11.3898	15.05531	20.82544	8.92289	54.92797	17.42808	22.00864	10.69978	49.8635
4	10.97836	6.66477	63.31843	17.85763	16.18429	18.55815	11.3268	53.36918	16.42891	20.07229	19.69236	43.80644
25	16.57056	23.67269	21.89644	36.96699	16.80594	21.4532	14.15183	46.97772	18.12607	22.8095	21.85279	37.21164
35	15.50647	24.97818	18.98742	40.41445	7.32641	40.63959	3.43663	48.03585	18.49186	23.11639	21.77866	36.61308
45	13.08073	29.26617	15.21459	42.25135	7.60523	40.1456	14.02694	37.69981	16.71993	23.7174	24.25682	35.30585
55	14.23667	31.43521	11.58036	42.51812	7.9367	41.61389	10.76433	39.19593	22.51814	20.95386	19.43635	37.09164
65	21.05222	53.69482	0.18181	25.07115	9.985	39.92767	12.07791	37.50638	14.74438	44.10907	2.65523	38.49132

Reference:

1 W. J. Sun, J. J. Vallooran, A. Zabara and R. Mezzenga, Nanoscale, 2014, 6, 6853.

2 W. J. Sun, J. J. Vallooran and R. Mezzenga, Langmuir, 2015, 31, 4558.

3 W. J. Sun, J. J. Vallooran, W. K. Fong and R. Mezzenga, J. Phys. Chem. Lett., 2016, 7, 1507.

4 J. Briggs, H. Chung, M. Caffrey, J. Phys. II 1996, 6, 723-751.